

Response Analysis of Nuclear Power Plants with Uplifting Basemats by Impulsive Green's Function Method

T. Nagano, A. Kowada, M. Ozaki
Kansai Electric Power Corporation, Inc., Osaka, Japan

J. Terada
New Japan Engineering Consultants Inc., Osaka, Japan

H. Kase
Tajimi Engineering Services, Ltd., Tokyo, Japan

INTRODUCTION

Basemat uplifting is frequently found in the seismic analysis of nuclear power plants, when they are subjected to strong earthquake excitations. This phenomenon causes significant changes in the dynamic response characteristics of structures. In recent years, many studies have been carried out on this problem with analytical and experimental approaches. We also have studied this problem(Ref.1). Our experimental results implied that the rocking and the sway damping ratios tended to increase with basemat uplifting. But some considerations for the aseismic design have led to that the damping ratio associated with uplifting basemats should be decreased with decreasing contact area of the basemat.

Analytical studies concerning the basemat uplifting have usually conducted by using a Winkler foundation model. But, this model will not be suitable to obtain the damping which may vary with the magnitude of the basemat uplift. In considering the rocking and sway dampings, it is essential to evaluate the radiation damping, which is generated by the waves propagating from the basemat to the surrounding soil and decays the basemat motion itself. Hence, it is desirable that a method follows the wave propagation approach. But, the established methods normally treat only linear problems in the frequency domain and cannot treat nonlinear problems which require the time domain analysis. Thus, the impulsive Green's function method(I.G.M.) has been developed to make it possible to perform the time domain analysis of the soil-structure interaction on a basis of 3-dimensional wave propagation theory for a homogeneous elastic halfspace. This method can also treat the basemat uplift.

This paper presents an analysis by the impulsive Green's function method and furthermore describes the rocking and sway damping properties influenced by the basemat uplifting.

ANALYTICAL METHOD

Let a unit step function of a vertical point loading P be acted on the origin placed on the surface of a homogeneous elastic halfspace, as shown in Fig. 1. Then, the vertical displacement at a point on the surface with a distance r from the loading point is given by (Ref.2)

$$w(r,t) = \frac{1-\nu}{2\pi G} \frac{P}{r} W(\tau) \quad (1)$$

where ν is the poisson's ratio of the halfspace, G is the shear modulus and τ is the dimensionless time which is designated by $V_s t/r$, where V_s = shear wave velocity.

Likewise, when a unit step function of a horizontal loading Q is applied at the origin, the resulting horizontal displacement in the loading direction at a point on the surface with a distance r is written as

$$u(r, \phi, t) = \frac{1}{2\pi G} \frac{Q}{r} \left[U(x) \cos^2 \phi + (1-\nu) V(x) \sin^2 \phi \right] \quad (2)$$

The displacement functions $W(x), U(x), V(x)$ represent the travel-time curves of the wave propagation and is found to become constants after the Rayleigh waves arrive in, as shown in Fig.2.

When the vertical point loading is given by a time function $P(t)$, the resulting response at a point on the surface is given by the Duhamel's integral:

$$w(r, t) = \frac{1-\nu}{2\pi G} \cdot \frac{1}{r} \int_0^t P(t-\ell) \frac{dW\left(\frac{Vs\ell}{r}\right)}{d\ell} d\ell \quad (3)$$

For numerical calculation, Eq.(3) can be rewritten in the discretized form,

$$w(r, n\Delta t) = \frac{1-\nu}{2\pi G} \cdot \frac{1}{r} \sum_{k=0}^{n'} H^z(r, k\Delta t) \cdot P[(n-k)\Delta t] \quad (4)$$

where

$$H^z(r, k\Delta t) = \frac{1-\nu}{2\pi G} \cdot \frac{1}{r} [W(r, (k+1/2)\Delta t) - W(r, (k-1/2)\Delta t)] \approx \frac{1-\nu}{2\pi G} \cdot \frac{1}{r} [W(r, (k+1)\Delta t) - W(r, k\Delta t)] \quad (5)$$

n' = minimum positive integer, for which the Rayleigh wave arriving time $t_R < n'\Delta t$

where $H^z(r, k\Delta t)$ represents the impulsive Green's function.

Especially, the displacement at the loading point itself may be given by

$$w(0, n\Delta t) = \frac{1-\nu}{\pi G r_0} \cdot P(n\Delta t) \quad (6)$$

where the displacement is approximated by that at the center of circle of radius r_0 , when the circle is subjected to a uniform loading. When, Eq.(6) is applied to a rectangular element, r_0 may be replaced by $A/\sqrt{\pi}$, A : area of the rectangular element. When the horizontal point loading is given by the time function $Q(t)$, the resulting response may be obtained in the similar form by using Eq.(2),

$$u_x(r, \phi, n\Delta t) = \sum_{k=0}^{n'} H^x(r, \phi, k\Delta t) \cdot Q((n-k)\Delta t) \quad (7)$$

where $H^x(r, \phi, k\Delta t)$ denotes the impulsive Green's function for horizontal loading.

For the numerical purpose, the bottom surface of the basemat and the relating contact surface of the soil are divided equally into numerous elements, each of which is represented by a node located at the center of the element, as shown in Fig.3. Then, the displacement w_{jn} of the soil element j at the time $n\Delta t$ can be obtained by the summation of the individual displacement due to the loading $P_{i, n-k}$ acted on the contact element i , as given by Eq.(4),

$$w_{jn} = \sum_{i=1}^m \sum_{k=0}^{n'} H^z_{ji, k} \varepsilon_{i, n-k} P_{i, n-k} \quad (8)$$

where $H^z_{ji, k} = H^z(r_{ji}, k\Delta t)$, $P_{i, n-k} = P_i((n-k)\Delta t)$, $P_{i, 0}$ = reaction at rest

$\varepsilon_{i, n-k} = \begin{cases} 0 & \text{when the basemat element is uplifting from the soil element,} \\ 1 & \text{when the basemat element contacts with the soil element,} \end{cases}$
 m = total number of elemens.

As found later, the present analysis requires an iterative calculation for evaluating whether an element contacts or uplifts during any time steps. To do this, it is useful to divide the soil displacement $w_{jn}^{(a-1)}$ into \bar{w}_{jn} due to past and known loadings until $(n-1)\Delta t$ and $\hat{w}_{jn}^{(a-1)}$ due to the presently applied and

known loading until the iteration step I-1. Since \hat{w}_{jn} has no relation with the iteration, one can write

$$w_{jn}^{(I-1)} = \tilde{w}_{jn} + \hat{w}_{jn}^{(I-1)}, \quad \tilde{w}_{jn} = \sum_{i=1}^m \sum_{k=1}^{n'} H_{ji,k}^z \varepsilon_{i,n-k} P_{i,n-k}, \quad \hat{w}_{jn}^{(I-1)} = \sum_{i=1}^m H_{ji,0}^z \varepsilon_{i,n}^{(I-2)} P_{i,n}^{(I-2)}, \quad P_{i,n}^{(1)} = 0 \quad (9)$$

(I) = iteration counter (= 1, 2, ...)

Similarly, the horizontal displacement of the soil element j is given by

$$u_{jn}^{(I-1)} = \tilde{u}_{jn} + \hat{u}_{jn}^{(I-1)}, \quad \tilde{u}_{jn} = \sum_{i=1}^m \sum_{k=1}^{n'} H_{ji,k}^x \varepsilon_{i,n-k} Q_{i,n-k}, \quad \hat{u}_{jn}^{(I-1)} = \sum_{i=1}^m H_{ji,0}^x \varepsilon_{i,n}^{(I-2)} Q_{i,n}^{(I-2)}, \quad Q_{i,n}^{(1)} = 0 \quad (10)$$

In the above, it is clear that the contact or uplift condition $\varepsilon_{in}^{(I-2)}$ is specified by

$$\varepsilon_{in}^{(I-2)} = 0 \text{ for } w_{in}^{(I-2)} < w_{in}^{(I-2)}; 1 \text{ for } w_{in}^{(I-2)} \geq w_{in}^{(I-2)} \quad (11)$$

On the other hand, the displacement $w_{in}^{(I-1)}$ of the basemat element i has been obtained by solving the concerned equation of motion at the iteration (I-1), so that the increments of the reactive forces $\Delta P_{jn}^{(I-1)}$ and $\Delta Q_{jn}^{(I-1)}$ may be estimated by

$$\Delta P_{jn}^{(I-1)} = a \frac{\pi Gr_0}{1-\nu} \varepsilon_{jn}^{(I-1)} (w_{jn}^{(I-1)} - w_{jn}^{(I-1)}), \quad \Delta Q_{jn}^{(I-1)} = a \frac{2\pi Gr_0}{2-\nu} \varepsilon_{jn}^{(I-1)} (u_{jn}^{(I-1)} - u_{jn}^{(I-1)} - u_{jl}^f + u_{jl}^i) \quad (12)$$

where a denotes the control factor for convergence and Δt is the time closest to $n\Delta t$, at which the contact has started again at element j . These provide

$$P_{jn}^{(I-1)} = P_{jn}^{(I-2)} + \Delta P_{jn}^{(I-1)}, \quad Q_{jn}^{(I-1)} = Q_{jn}^{(I-2)} + \Delta Q_{jn}^{(I-1)}, \quad P_{jn}^{(1)} = 0, \quad Q_{jn}^{(1)} = 0 \quad (13)$$

Hence, the resultant reactive force vectors are obtained by

$$\begin{aligned} \{R\}_n^{(I-1)} &= (\{R_h, R_v, R_\theta\}_n^T)^{(I-1)} \\ R_{hn}^{(I-1)} &= \sum_j \varepsilon_{jn}^{(I-1)} Q_{jn}^{(I-1)}, \quad R_{vn}^{(I-1)} = \sum_j \varepsilon_{jn}^{(I-1)} P_{jn}^{(I-1)}, \quad R_{\theta n}^{(I-1)} = \sum_j y_j \varepsilon_{jn}^{(I-1)} P_{jn}^{(I-1)} \end{aligned} \quad (14)$$

Now, consider the displacement vector $\{u^{bm}\}_n$ of the basemat and $\{u\}_n$ of the total system including the superstructure and basemat, which are defined by

$$\{u^{bm}\}_n^{(I)} = (\{u_h, u_v, \theta\}_n^T)^{(I)}, \quad \{u\}_n^{(I)} = \begin{bmatrix} \{u^{ss}\} \\ \{u^{bm}\} \end{bmatrix}_n^{(I)} \quad (15)$$

and illustrated in Fig.4. Herein, the basemat displacements are related to the basemat element displacements by the following equations

$$u_{jn}^{f(I)} = u_{hn}^{(I)}, \quad w_{jn}^{f(I)} = u_{vn}^{(I)} + y_j \theta_n^{(I)} \quad (16)$$

where y_j = y-coordinate of the element j .

For keeping the rapid convergence of iterative calculation, it is useful to transform the equation of motion to

$$[M]\{\ddot{u}\} + [C]\{\dot{u}\} + [K]\{u\} + (\{R\} - [K]\{u\}) = -[M]\{\ddot{u}_g\} \quad (17)$$

where

$$[K] = \text{diag}[K_h, K_v, K_\theta] \quad (18)$$

$$K_h = \sum_j \frac{2\pi Gr_0}{2-\nu}, \quad K_v = \sum_j \frac{\pi Gr_0}{1-\nu}, \quad K_\theta = \sum_j \frac{\pi Gr_0}{1-\nu} y_j$$

$[M]$ = mass matrix, $[C]$ = damping matrix, $\{\ddot{u}_g\}$ = excitation vector.

The response analysis of the structure and the basemat will be performed by using the Newmark's method,

$$\{u\}_n^{(I)} = \{u\}_n^{(I-1)} + \{\Delta u\}_n^{(I)}, \quad \{u\}_n^{(I)} = \{u\}_{n-1} + \Delta t \{\dot{u}\}_{n-1} + \Delta t^2/2 \cdot (1-2\beta) \{\ddot{u}\}_{n-1} \quad (19)$$

$$\{\dot{u}\}_n^{(I)} = \{\dot{u}\}_n^{(I-1)} + \Delta t \gamma \{\ddot{u}\}_n^{(I)}, \quad \{\dot{u}\}_n^{(I)} = \{\dot{u}\}_{n-1} + \Delta t(1-\gamma) \{\ddot{u}\}_{n-1}, \quad \{\ddot{u}\}_n^{(I)} = (\{u\}_n^{(I)} - \{u\}_n^{(I-1)})/(\Delta t^2 \beta)$$

$$\{\Delta u\}_n^{(I)} = ([K^*])^{-1} \{\Delta R\}_n^{(I-1)}, \quad [K^*] = [M]/(\Delta t^2 \beta) + \gamma [C]/(\Delta t \beta) + [K] \quad (20)$$

$$\{\Delta R\}_n^{(I-1)} = -[M]\{\ddot{u}_g\}_n - [M]\{\ddot{u}\}_n^{(I-1)} - [C]\{\dot{u}\}_n^{(I-1)} - \{R\}_n^{(I-1)} \quad (21)$$

and the iteration calculation proceeds as follows:

- (i) Calculate $\{\Delta u\}_n^{(0)}$ using Eq.(20),
- (ii) Calculate $\{u\}_n^{(0)}$, $\{\dot{u}\}_n^{(0)}$, $\{\ddot{u}\}_n^{(0)}$ by using the results of (i) and Eq.(19),
- (iii) Obtain $\{\Delta R\}_n^{(0)}$ by substituting the above results into Eq.(21),
- (iv) Return to (i).

When the convergence

$$(\| \{\Delta R\} \|_n^{(0)} - \| \{\Delta R\} \|_n^{(i-1)}) / \| \{R\} \|_n^{(0)} \rightarrow 0 \quad (22)$$

is completed, the time step n is replaced by $n+1$.

SIMULATION ANALYSIS

A response analysis was carried out to simulate a shaking table test of a rigid structure model supported on a silicon rubber soil model when it was subjected to sinusoidal excitation. The size of the model was 1.0m × 1.0m in plan and 0.2m thick. The modulus of elasticity of the silicon rubber of the soil model was about 10kgf/cm² and its density was 1.5gf/cm³. The structure model was rigidly made of acrylic resin, as shown in Fig.5. This model on the soil had the first mode natural frequency of about 5.0Hz. The three acceleration levels of input excitation were applied, these were 10, 30, 50 cm/sec² respectively.

In the analysis, the mesh discretization of the contact area is shown in Fig.6. Although the experimental soil model had the limited volume, the analysis treated this as an halfspace. The analysis considered the coupled motion of rocking, vertical and sway motions. The resonance curves obtained by using the I.G.M. is shown in Fig.7, in comparison with the experimental results. The corresponding ratio which is the ratio of the maximum uplifting area during one cycle to the whole base area is shown in Fig.8. It is found that the analytical results considerably agreed with the experimental results.

EVALUATION OF ROCKING AND SWAY DAMPING

The damping can be evaluated by the area of hysteresis loops, which indicate the relation between the reactive force and the displacement of the basemat. In the present study, the damping ratio h was computed by using the above simulation analysis results in accordance with the well known equation:

$$h = \frac{1}{4\pi} \cdot \frac{\Delta E}{E} \quad (23)$$

where ΔE : energy loss given by the area of loop,

E : potential energy given by the area enclosed by the displacement axis and the backbone curve in their one side as shown in Fig.9

The obtained damping ratio of rocking and sway are shown in Fig.10, where the ratio of the damping ratio of the uplifting basemat to that of the full contacted mat (linear) is given as functions of the contact ratio of the minimum contact area during one cycle to the whole area of the basemat. It is found that the rocking damping ratio considerably increased with decrease of the contact ratio. This increase is supposed to have produced by the increasing contribution of the vertical impedance arising from uplifting of the basemat. The sway damping indicated no significant increase with increase of uplift of the basemat.

CONCLUSIONS

The impulsive Green's function method indicated a good prediction for a model shaking table test of uplifting basemats. Thus, it seems that this method will be effective to treat other separation problems exhibited in the soil-structure interaction as well as basemat uplifting accompanied by structural nonlinear response. The rocking damping ratio computed by the I.G.M. showed a tendency of increase with increasing uplift of the basemat. This problem seems to be valuable to a further study.

REFERENCES

(1) Setogawa, S., et al., (1987), "Study on the Seismic Stability of a Power Plant Structure and Foundation (1) (2)", SMIRT 9, k1, pp.285-296.

(2) Shimomura, Y. and Tajimi, H., (1986), "On an Estimation of the Radiation Damping in Uplift Motions", Journal of structure and construction engineering, Architectural Inst. of Japan, Nov.

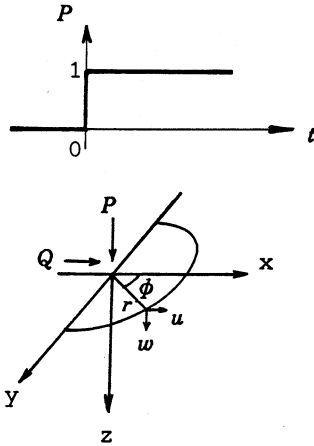


Figure 1. Unit step function

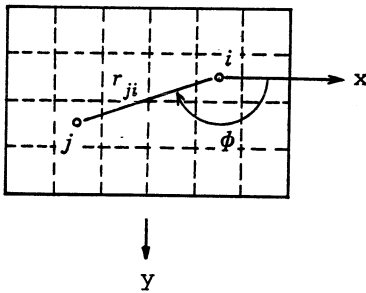


Figure 3. Bottom surface of base mat

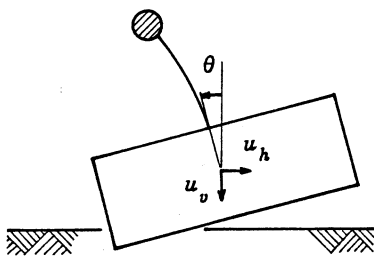


Figure 4. Coordinate system of structure

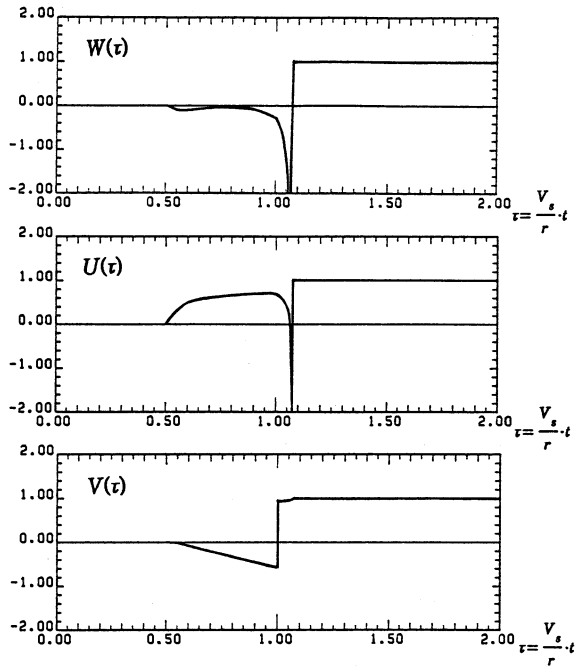


Figure 2. Displacement function due to unit step loading

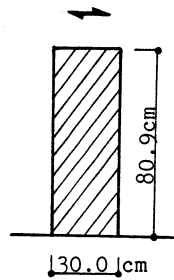


Figure 5. Rigid structure model

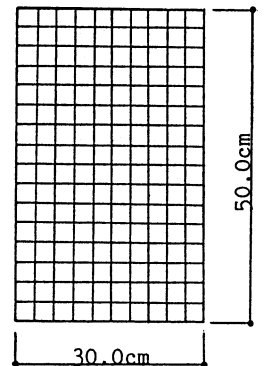


Figure 6. Element of mat surface of analytical model

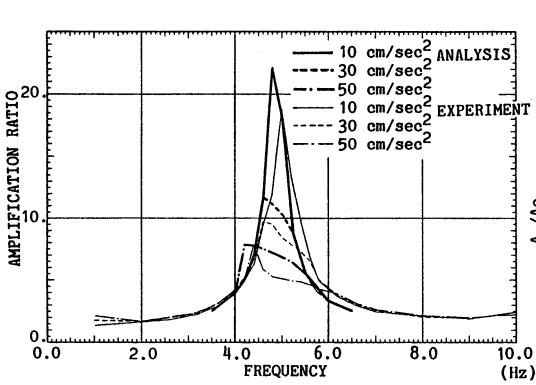


Figure 7. Resonance curves

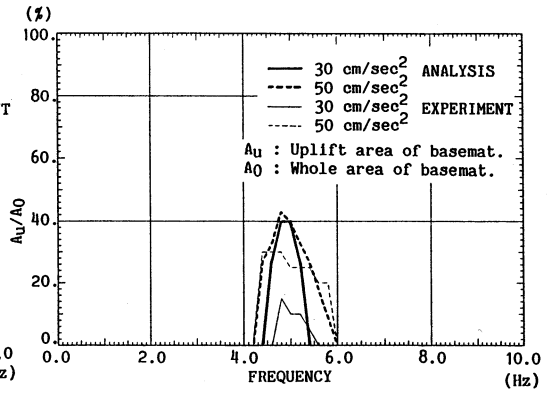


Figure 8. Uplift ratio

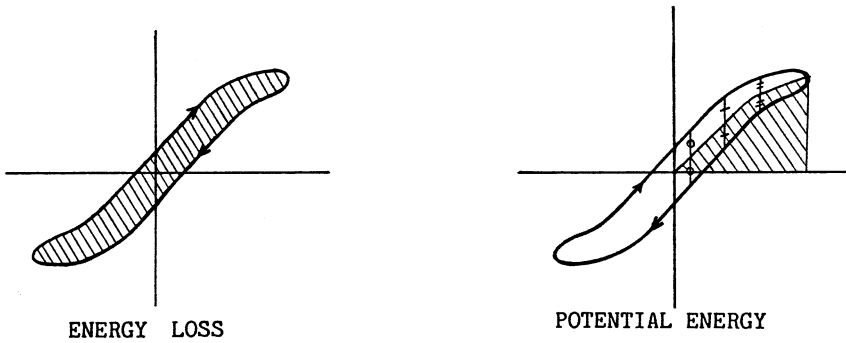


Figure 9. Hysteresis loop

h : Damping ratio. A_c : Contact area of basemat.
 h_0 : Damping ratio of linear response. A_0 : Whole area of basemat.

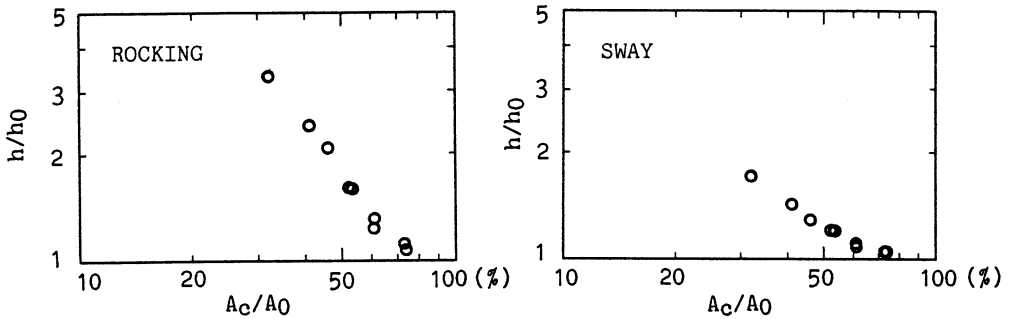


Figure 10. Relationship between h/h_0 and A_c/A_0